18TH WORLD CONFERENCE ON EARTHQUAKE ENGINEERING
WCEE2024
MILAN

MILAN, ITALY
30TH JUNE - 5TH JULY 2024
www.wcee2024.it

NON-LINEAR SITE EFFECTS IN AREAS CHARACTERISED BY A COMPLEX TOPOGRAPHY: AN ITALIAN CASE STUDY

G. Falcone[1,2], G. Elia[2], A. di Lernia[2] & F. Cafaro[2]

[1] University of Napoli Federico II, Napoli, Italy (gaetano.falcone@unina.it)

[2] Technical University of Bari, Bari, Italy

Abstract: *The paper presents the application of a three-dimensional (3D) finite element (FE) non-linear approach to assess the site effects in areas characterised by complex topography. In particular, the seismic response of the Costa del Canneto area, located in the southern Apennines of Italy, is investigated. This region is known for its high base seismic hazard. The presence of soft soils reaching depths up to 200 meters could considerably affect the earthquake amplification at ground surface. To capture the local topographic conditions with reliable accuracy, a 3D FE model is generated from the Digital Terrain Model. In the presented preliminary analyses, the soil deposit is considered homogeneous with depth, characterised by a constant shear wave velocity of 400 m/s and overlying a deep horizontal seismic bedrock. To highlight the effects of soil non-linearity on the ground surface motion, the soil behaviour is described through linear visco-elastic and visco-elastic perfectly plastic schemes, but also implementing the Hardening Soil model with small strain stiffness. The horizontal components of the same reference earthquake, selected according to the base seismic hazard of the site, are simultaneously applied at the base of the FE model. The results of the simulations provide a detailed understanding of the seismic behaviour of the Costa del Canneto area, considering the interaction between the soft soil layers and the topographic irregularities. The case study represents a significant step forward in the analysis of site effects in complex geo-mechanical contexts, such as those occurring in the Italian southern Apennines. Indeed, it can promote the use of advanced seismic hazard assessments for an effective seismic risk mitigation in similar geo-mechanical settings.*

1. Introduction

It is known that the seismic shaking at surface depends on local topographic and stratigraphic conditions. For sites where stratigraphic amplification phenomena are expected, such as those with a horizontal stratigraphy, the study of local seismic response (LSR) can be based on a one-dimensional (1D) approach (Gazetas, 1982; Amorosi et al., 2016; Régnier et al., 2018). Instead, in the presence of complex topography or buried geometries, two- and three-dimensional models (2D and 3D, respectively) should be generated for LSR computations (Jibson, 1987; Geli et al., 1988; Rizzitano et al., 2014; Falcone et al., 2018; Moczo et al., 2018; di Lernia et al., 2023). Regarding simplified 2D geometries, the literature provides solutions for a preliminary estimation of the expected topographic effect on LSR based on parameters that synthetically represent both the geometry and the material characterising the site (Bouckovalas & Papadimitriou, 2005; Gatmiri & Arson, 2008). Moreover, machine learning approaches have been recently employed by various authors (Mori et al., 2021; Zhu et al., 2022) for large-scale prediction of ground shaking, encompassing both topographic and stratigraphic effects. However, for particularly complex topographies requiring 3D models, a parametric

analysis should be performed to assess the effect of the accuracy of the 3D model itself on LSR results (Falcone et al., 2023).

In this context, 3D LSR analyses have been conducted using a FE code with reference to a prototype case characterised by a complex geo-mechanical and topographic setting. To highlight the solely topographic effect on surface shaking, no buried morphologies or variations in shear wave velocity with depth have been implemented in the 3D FE models. Moreover, different numerical simulations of the same case study have been conducted by varying the constitutive model assumed for the soil above the seismic bedrock. Specifically, a linear visco-elastic, a linear visco-elastic perfectly plastic and a non-linear elasto-plastic model have been considered to simulate the soil deposit dynamic response. The numerical simulation setup enables the assessment of the effects of soil constitutive modelling, specifically focusing on plasticity and non-linearity, on the ground surface shaking in the area with uneven topography.

The results at the ground surface are presented in terms of amplification factors (AFs), determined according to the following equations:

$$AF_{PGA} = \frac{PGA_o}{PGA_r} \tag{1}$$

$$AF_{T1-T2} = \frac{\int_{T1}^{T2} Sa_o(T)dT}{\int_{T1}^{T2} Sa_r(T)dT} \tag{2}$$

where the subscripts "o" and "r" refer, respectively, to the output signal obtained at the ground level through LSR analysis and the reference signal, PGA is the Peak Ground Acceleration, T is the spectral period and T1-T2 is the range of periods adopted for the integration of the acceleration response spectra, Sa(T).

2. The Costa del Canneto case study

The Costa del Canneto area (Matera, Italy) is located in the Basilicata region, within the Italian southern Apennines. The site of reference is crossed by the Alvaro tunnel (AT) near Ferrandina Scalo. Figure 1a shows the Digital Terrain Model (DTM) of the area of interest (with a cell size of 5 m) and the location of the Alvaro tunnel. The DTM has been obtained from the regional administration website (Basilicata, 2022). The area features a 3D uneven topography (Figure 11b). Thus, a complex dynamic site response is expected to significantly influence the ground motion modification pattern in the area. Specifically, a primary slope is identified in the SW-NE direction, with additional local slopes spread along the NW-SE direction.

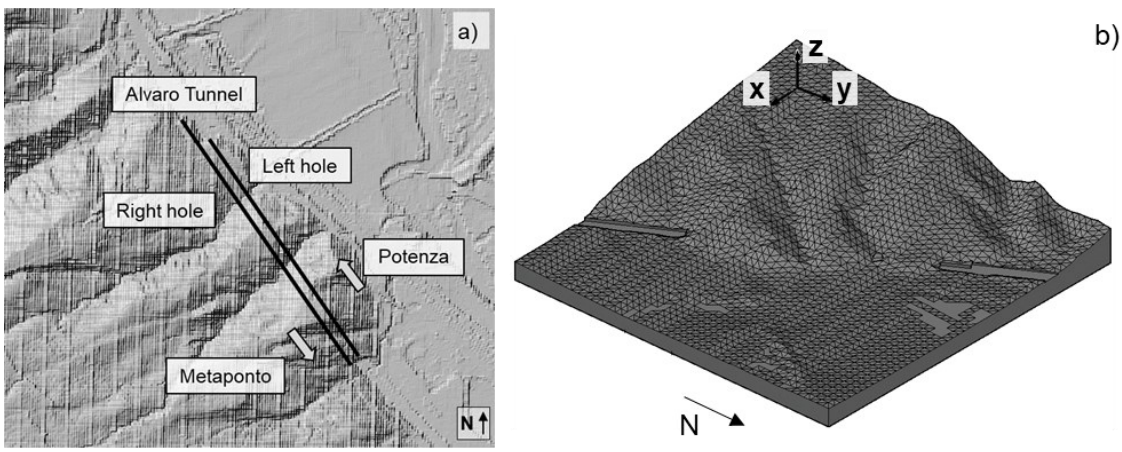

Figure 1. Costa del Canneto slope: a) DTM and b) three-dimensional model adopted for LSR analyses.

The reference seismic hazard is displayed in Figure 2a in terms of PGA distribution for a return period (T_R) of 1898 years, corresponding to a probability of exceedance of 10% in 200 years according to the class of use of tunnels and a limit state of life safety.

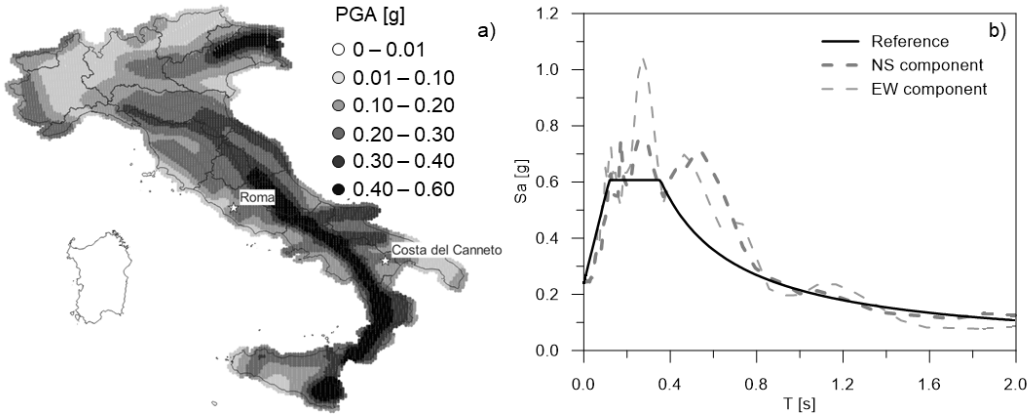

Figure 2. Reference seismic hazard in terms of a) map of PGA and b) pseudo-spectral acceleration for a return period of 1898 years.

The reference hazard has been defined in terms of response spectrum of the pseudo-accelerations for a class A site (i.e., flat outcropping rock) with T_R = 1898 years (Figure 2b), according to the ItBC (2018) and referring to the study by Meletti and Montaldo (2007), Montaldo and Meletti (2007) and Stucchi et al. (2011). The NS and EW components of the earthquake recorded at Cascia (PG, Italy) on the 14th October 1997, available at https://itaca.mi.ingv.it/ItacaNet_32/#/station/IT/CSC, have been selected as input motions since they are characterised by a low value of the average root-mean-square deviation of the observed spectrum from the target design spectrum, D_{rms}, defined as:

$$D_{rms} = \frac{1}{N}\sqrt{\sum_{i=1}^{n}\left(\frac{Sa_{real}(T_i)}{PGA_{real}} - \frac{Sa_{ref}(T_i)}{PGA_{ref}}\right)} \quad (3)$$

where N is the number of considered spectral periods, Sa is the spectral acceleration, PGA is the peak ground acceleration. Moreover, the subscripts “real” and “ref” are referred to the selected accelerograms and the reference spectrum, respectively. The smaller is the value of D_{rms}, the closer is the match between the shape of the selected signals and the target spectrum. Both signals have been scaled to the peak ground acceleration of the reference spectrum, equal to 0.24 g, and their response spectra are plotted in Figure 2b.

3. Numerical model

The three-dimensional FE model (Figure 1b), implemented in PLAXIS 3D (Brinkgreve et al., 2022), incorporates an accurate representation of the topography of the area and accounts for the presence of two tunnel openings representing the Alvaro tunnel. A homogeneous deposit (i.e., shear wave velocity, V_S, constant with depth) with irregular topography overlying the seismic bedrock (V_S = 800 m/s) has been considered. The position of the seismic bedrock has been assumed to coincide with the base of the numerical model. Three main phases have been simulated in the numerical analysis: initially, the stress state has been initialised using the gravity loading option (phase 1); subsequently, a static phase, involving the activation of the tunnel lining and deactivation of the soil elements inside the tunnel has been considered (phase 2). In the third and last phase, the seismic input motions have been applied at bedrock (phase 3). The water table has been assumed at the base of the FE model, considering a soil drained behaviour for simplicity. Standard boundary conditions have been applied during the static stages (i.e., no horizontal displacement along the vertical sides and fully fixed displacements at the base of the model). During the dynamic phase, free-field boundary conditions have been used along the vertical sides and a compliant base has been adopted at the model base. The compliant base condition facilitates the propagation of the outcropping reference signals as input motions from the base of the FE model. On the other hand, the free-field condition prevents the reflection of unwanted seismic waves along the vertical boundaries of the model. The dynamic simulations have been conducted with a time step matching that of the two reference horizontal components of the input signal, which have been simultaneously applied at the base of the FE model.

As the objective of this work is to explore the impact of soil dynamic behavior on the seismic response predicted at ground surface, three different constitutive models have been considered for the ideal homogenous soil deposit: a simple linear visco-elastic, a linear visco-elastic perfectly plastic and a non-linear elasto-plastic model (referred to as LE, LEP, and NL, respectively). The non-linear cyclic behaviour has been accounted for by means of the Hardening Soil model with small strain stiffness (HSsmall), developed by Schanz et al. (1999). The material properties for the soil, including unit weight (γ_t), shear wave velocity (V_S), Poisson's coefficient (ν'), effective cohesion (c'), and friction angle (ϕ'), have been assumed constant with depth and equal to 20 kN/m^3, 400 m/s, 0.25, 22.6 kPa, and 25.1°, respectively. Instead, the relevant HSsmall model parameters are outlined in Table 1, while the decay of the normalized shear stiffness modulus (G/G_0) and the increase of the damping ratio (D) with shear strain (γ) implemented through the HSsmall model are shown in Figure 3. The HSsmall model has been calibrated to replicate a stiffness decay and hysteretic dissipation consistent with the G/G_0 and D curves proposed by Darendeli (2001), as depicted in Figure 3. A small amount of Rayleigh damping (0.01%) associated with frequencies of 1 and 10 Hz has also been introduced in the dynamic analyses to prevent zero dissipation at very low strain levels. It should be noted that the soil parameters for both the linear visco-elastic (i.e., γ_t, V_S and ν') and linear visco-elastic perfectly plastic (i.e., γ_t, V_S and ν', c' and ϕ') models have been selected to align with the HSsmall model parameters. The bedrock material at the base of the FE models has been treated as linear visco-elastic, with values for the unit weight (γ_t), shear wave velocity (V_S), Poisson's coefficient (ν') and damping ratio set equal to 20 kN/m^3, 800 m/s, 0.25, and 0.01%, respectively.

Table 1. HSsmall model parameters.

Parameter	Description	Value
c' [kPa]	Effective cohesion	22.6
φ' [°]	Effective friction angle	25.1
ψ [°]	Dilatancy angle	0
E_{50}^{ref} [kPa]	Reference secant stiffness in standard drained triaxial test	52·E3
E_{oed}^{ref} [kPa]	Reference tangent stiffness for primary oedometer loading test	52·E3
E_{ur}^{ref} [kPa]	Reference unloading/reloading stiffness at engineering strains	157·E3
ν_{ur} [-]	Poisson's ratio for unloading/reloading	0.25
G_0^{ref} [kPa]	Reference shear modulus at very small strains	326·E3
m	Power for the stress-level dependency of stiffness	0
$\gamma_{0.7}$ [%]	Shear strain at which $G_S = 0.722 \cdot G_0^{ref}$	4·E-4
p'_{ref} [kPa]	Reference stress for stiffness	100
R [-]	Failure ratio	0.9
σ_{tens} [kPa]	Tensile strength	0

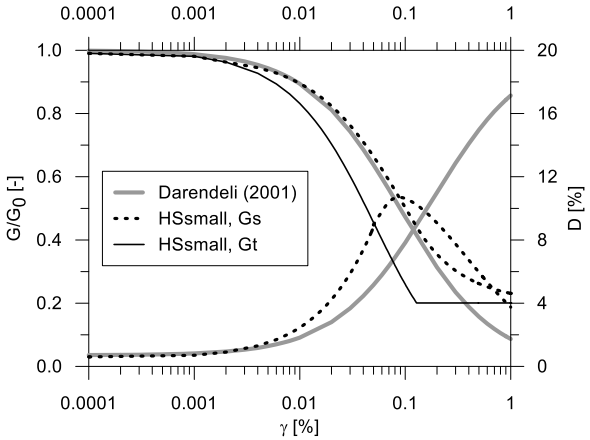

Figure 3. G/G_0 and D curves predicted by HSsmall.

4. Results

The numerical results are shown in Figure 4 for the LEP and NL analyses in terms of AF_{PGA} amplification maps of the seismic input along both horizontal directions. In the same figure, the topographic surface of the model is also depicted. For both LEP and NL models, higher values of AFs are distributed where local crests are located. Moreover, AFs peak values for the NL analysis are generally lower than those obtained from the LEP simulation. For a better understanding of the effect of the non-linear soil response on the ground motion amplification, scatter plots and correlation of AFs with elevation, z (where the elevation is the height of the ground surface with respect to the base of the numerical model) have been derived from the results, as shown next.

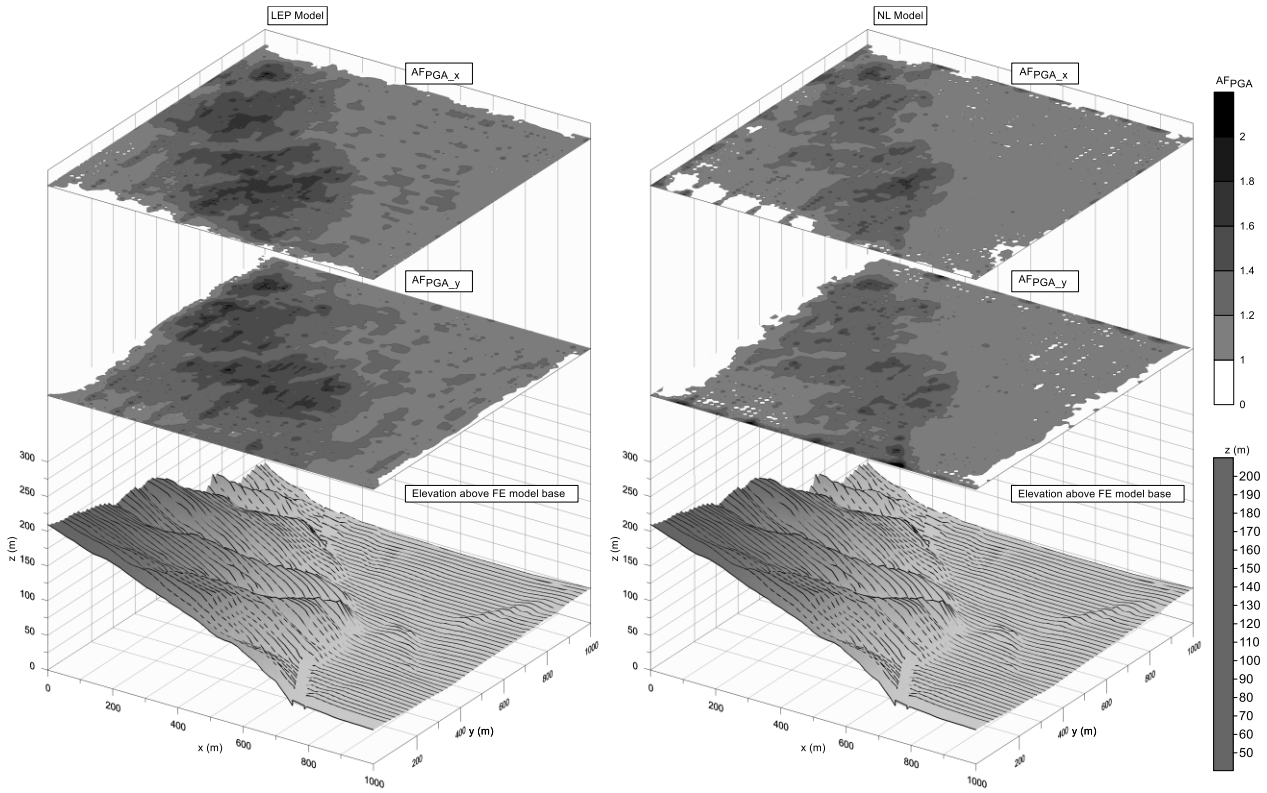

Figure 4. Amplification maps in terms of AF_{PGA} for LEP and NL analyses.

The scatter plots of the amplification with respect to z are shown in Figure 5a and Figure 5b, in terms of AF_{PGA} and $AF_{0.7\text{-}1.1}$, respectively. The AF-z scatter plots suggest a bell-shaped curve of correlation, while a higher dispersion is obtained for AF_{PGA}-z. Bearing in mind that V_S is constant with depth, these scatter plots show a rough correlation between the ground motion amplification and the topography of the area. Conversely, other proxies, such as the slope in the x or y direction of the model, result in very scattered diagrams without any significant correlation. As a preliminary attempt to show the effect of the constitutive model on the ground motion modification for area characterized by complex topography, the AF-z correlations shown in Figure 6 have been derived using a polynomial equation:

$$AF = a \cdot z^2 + b \cdot z + c \tag{4}$$

The values of the coefficients a, b, and c are not provided here for sake of brevity. It is worth noting that the peak values of AF_{PGA} are higher than the other AFs. In fact, AF_{PGA} for LE model are lower than the LEP and NL ones, while $AF_{0.1–0.5}$, $AF_{0.4–0.8}$, and $AF_{0.7–1.1}$ for the LE model are at least equal to or higher than the LEP and NL ones. This is because the earthquake has activated many plastic points in the 3D model, associated with the increase of PGA. Figure 7 show the plastic points activated during the initialisation of the model and the dynamic phase for the LEP and NL simulations, enlightening the initiation of local collapses induced by the seismic action, which cause the increase of PGA with respect to the LE analysis.

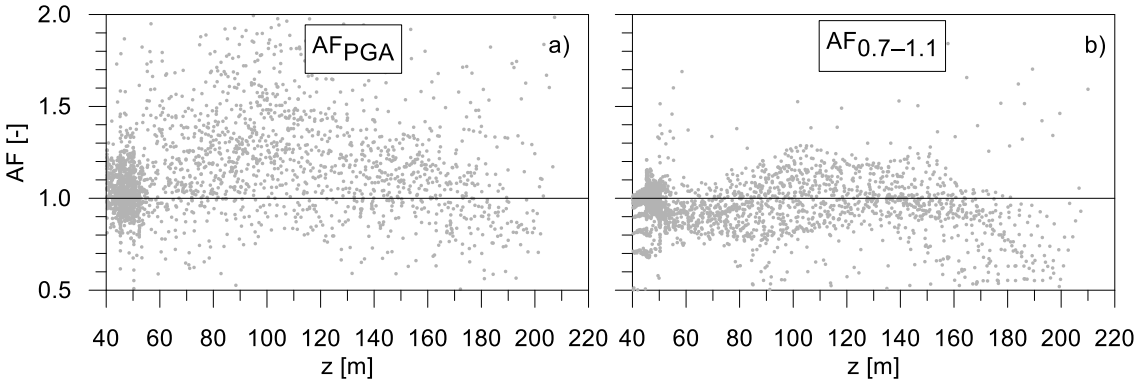

Figure 5. Scatter plots of a) AF_{PGA} and b) $AF_{0.7–1.1}$ with elevation.

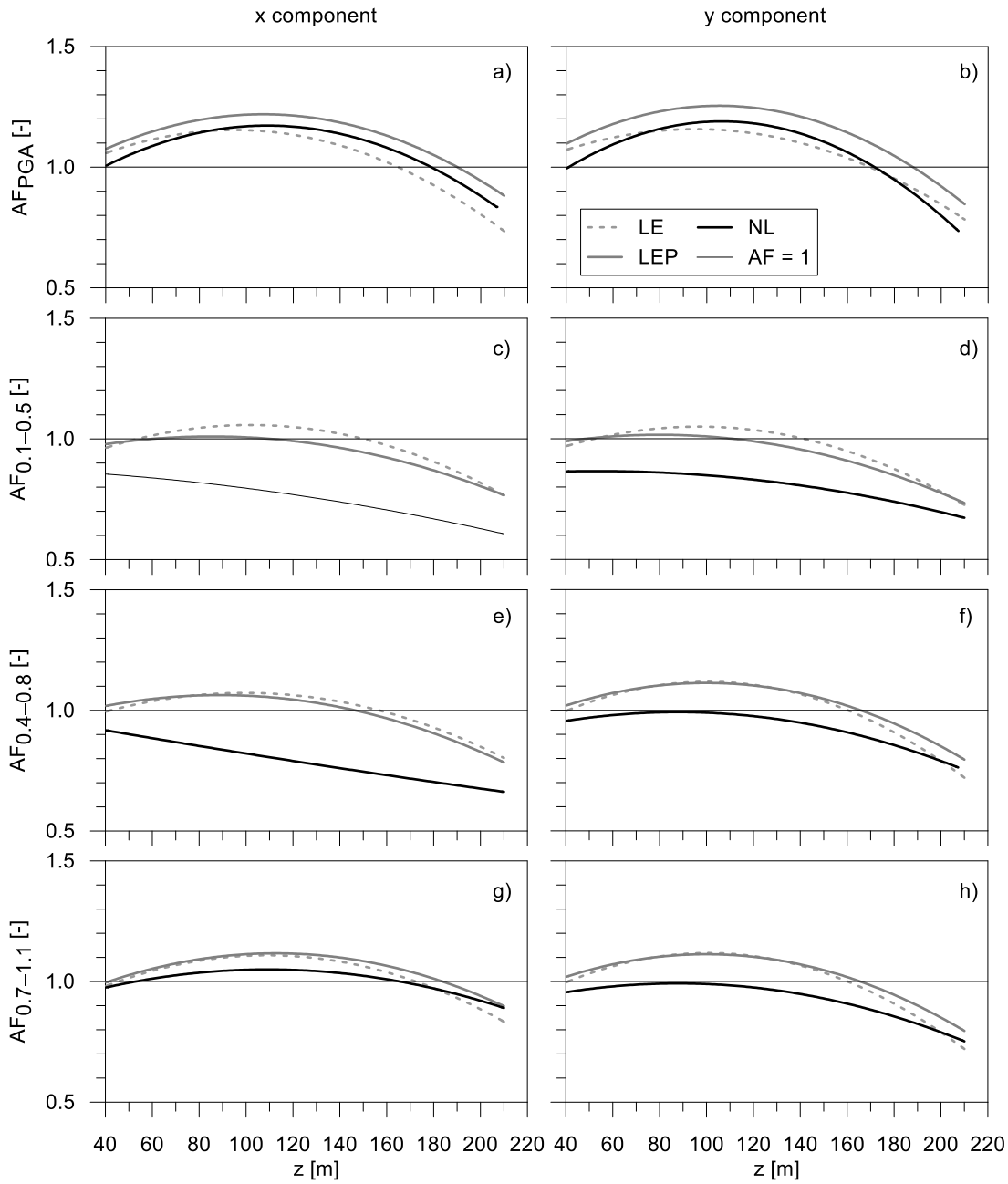

Figure 6. Correlation of AFs with elevation.

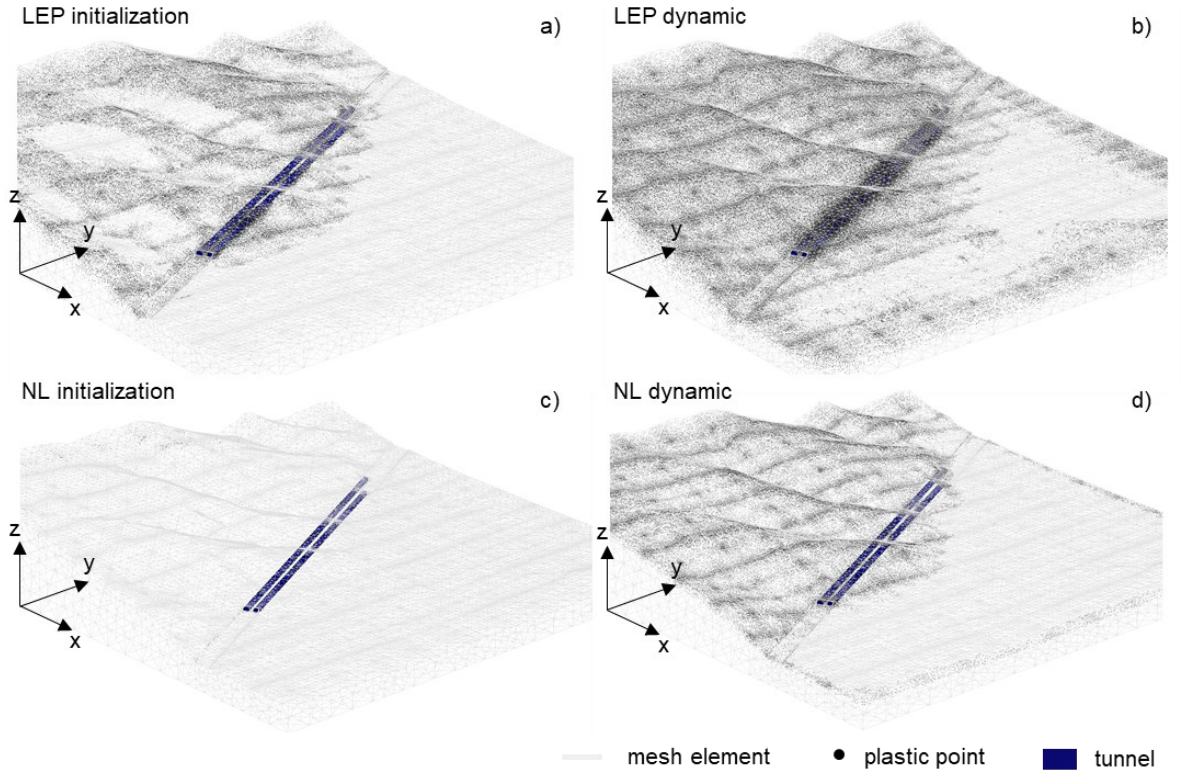

Figure 7. Plastic points activated during the gravity loading (left) and the dynamic phase (right) for a-b) the LEP and c-d) the NL analyses.

Finally, the differences between the AFs obtained from the NL and LEP analyses have been calculated through the following equation and shown in Figure 8:

$$\Delta AF = \frac{AF_{NL} - AF_{LEP}}{AF_{LEP}} \quad (5)$$

The mean value of the distribution of these differences is always smaller than -20%, which means that the AFs from NL analyses are generally lower than those from LEP simulations. The variability (i.e., the difference between the 75th and 25th percentiles) is about 20% for AF_{PGA} and less than 10% for the AFs in the three period intervals.

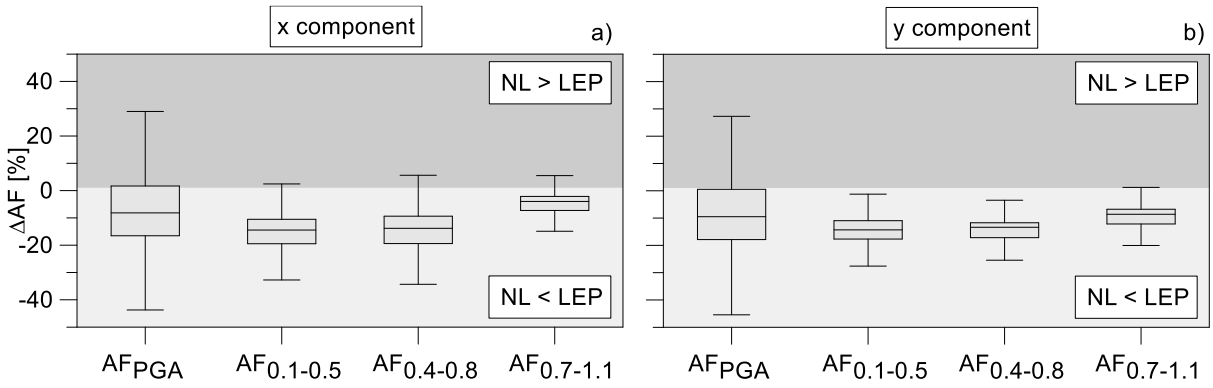

Figure 8. Box-plots of the error ΔAF referred to a) x and b) y components.

5. Conclusions

Preliminary results from a parametric study of local seismic response under complex topographic conditions are presented in this study. Starting from the DTM of the municipality of Ferrandina (Matera, Italy), a three-

dimensional model accurately reproducing the topography of the Costa del Canneto area has been constructed. The soil deposit has been assumed homogeneous, with a shear wave velocity constant with depth, and its dynamic behaviour has been simulated through a linear visco-elastic, a linear visco-elastic perfectly plastic and a non-linear elasto-plastic model. Consequently, three 3D numerical models have been analysed, at the base of which the two horizontal components of the reference signal have been simultaneously applied. The results of the dynamic simulations in terms of amplification factors reveal a complex response of the study area tied to the topographic irregularity and the selected constitutive model. It is important to note that the AFs have been determined for both the peak ground acceleration (PGA) and three spectral intervals, 0.1-0.5 s, 0.4-0.8 s, and 0.7-1.1 s. Furthermore, the AFs values have been correlated with the elevation of the ground level. The results of the investigation have shown that:

- for each elevation, there is a high variability of the AFs. For example, referring to the NL analysis and z = 100 m, AF_{PGA} varies between 0.8 and 2, while $AF_{0.7\text{-}1.1}$ varies between 0.5 and 1.3;
- the AF-z correlation exhibits a bell-shaped curve, having a peak at z approximately equal to 100 m for the study site;
- AF_{PGA} is generally higher compared to the amplification observed for the three selected period intervals. Additionally, concerning PGA, it is observed that the AFs from the LE analysis are lower than those from the LEP and NL analyses, whereas, for the three period intervals, the AFs from the LE analysis are higher than those resulting from the LEP and NL analyses. It is important to note that this is due to the local mobilisation of earthquake-induced permanent displacements, as confirmed by the plotting of plastic points at the end of the dynamic phase.

Finally, the differences between the AFs obtained from NL and LEP analyses have been calculated. It was observed that the mean value of the distribution of these differences is always less than -20% (i.e., AFs from NL analyses are lower than those from LEP simulations). The variability (i.e., the difference between the 75^{th} and 25^{th} percentiles of the errors distribution) is about 20% for AF_{PGA} and less than 10% for the AFs in the three period intervals.

In the future, the parametric analysis will be expanded to include subsurface stratigraphic heterogeneity as deduced from upcoming in-situ surveys and by selecting additional reference signals. The data collected from this parametric study may be valuable for training alternative and efficient techniques for both seismic shaking prediction and the design of decision support systems for managing structures and infrastructure in seismic areas.

6. Acknowledgments

Profs. Di Maio and Vassallo, from Università della Basilicata (Italy), are kindly acknowledge for the helpful discussion. The support received from the PON-MITIGO (ARS01_00964) project is also acknowledged. The first author is grateful for the financial support provided by the European Union - Next Generation EU, in the framework of the GRINS - Growing Resilient, INclusive and Sustainable project (GRINS PE00000018 - CUP E63C22002140007). The work is also part of the research activity developed by the second author within the framework of the PNRR CN MOST, SPOKE 7 “CCAM, Connected Networks and Smart Infrastructure” - WP4. The views and opinions expressed are solely those of the authors and do not necessarily reflect those of the European Union, nor can the European Union be held responsible for them.

7. References

Amorosi, A., Boldini, D., di Lernia, A., 2016. Seismic ground response at Lotung: Hysteretic elasto-plastic-based 3D analyses. *Soil Dynamics and Earthquake Engineering* 85, 44–61.

Bouckovalas, G.D., Papadimitriou, A.G. (2005). Numerical evaluation of slope topography effects on seismic ground motion. *Soil Dynamics and Earthquake Engineering* 25, 547–558.

Brinkgreve, R.B.J., Kumarswamy, S., Swolfs, W.M. (2022). PLAXIS 3D CONNECT Edition V22 Update 1.

Darendeli, M.B. (2001). Development of a new family of normalized modulus reduction and material damping curves. *Ph.D. Thesis*. University of Texas at Austin, USA.

di Lernia, A., Buono, C., Elia, G., 2023. Evaluation of seismic site effects in a real slope through 2D FE numerical analyses. *Proceedings of COMPDYN 2023, 9th International Conference on Computational Methods in Structural Dynamics and Earthquake Engineering*. 12–14 June. Athens, Greece.

Falcone, G., Boldini, D., Amorosi, A. (2018). Site response analysis of an urban area: A multi-dimensional and non-linear approach. *Soil Dynamics and Earthquake Engineering* 109, 33–45.

Falcone, G., Elia, G., Cafaro, F., di Lernia, A. (2023). Preliminary assessment of the correlation between three-dimensional topography and lining forces induced by earthquakes on shallow tunnels. *Proceedings of 10th European Conference on Numerical Methods in Geotechnical Engineering (NUMGE 2023)*. 26-28 June. London, England.

Gatmiri, B., Arson, C. (2008). Seismic site effects by an optimized 2D BE/FE method II. Quantification of site effects in two-dimensional sedimentary valleys. *Soil Dynamics and Earthquake Engineering* 28, 646–661.

Gazetas, G. (1982). Vibrational characteristics of soil deposits with variable wave velocity. *International Journal for Numerical and Analytical Methods in Geomechanics* 6, 1–20.

Geli, L., Bard, P.-Y., Jullien, B. (1988). The effect of topography on earthquake ground motion: A review and new results. *Bulletin of the Seismological Society of America* 78.

ItBC (2018). CS.LL.PP. Decreto Ministeriale: norme tecniche per le costruzioni. Gazzetta Ufficiale della Repubblica Italiana, n. 42, 20 febbraio, Suppl. Ordinario n. 8. Ist. Polig. Rome: e Zecca dello Stato S.p.a.

Jibson, R.W. (1987). Summary of research on the effects of topographic amplification of earthquake shaking on slope stability. *Report for USGS Numbered Series*. Mnlo Park, California.

Meletti, C., Montaldo, V. (2007). Stime di pericolosità sismica per diverse probabilità di superamento in 50 anni: valori di ag. Progetto DPC-INGV S1, Deliverable D2.

Moczo, P., Kristek, J., Bard, P.Y., Stripajová, S., Hollender, F., Chovanová, Z., Kristeková, M., Sicilia, D. (2018). Key structural parameters affecting earthquake ground motion in 2D and 3D sedimentary structures. *Bulletin of Earthquake Engineering* 16, 2421–2450.

Montaldo, V., Meletti, C. (2007). Valutazione del valore della ordinata spettrale a 1sec e ad altri periodi di interesse ingegneristico. Progetto DPC-INGV S1, Deliverable D3.

Mori, F., Mendicelli, A., Falcone, G., Acunzo, G., Spacagna, R.L., Naso, G., Moscatelli, M. (2021). Ground motion prediction maps using seismic microzonation data and machine learning. *Natural Hazards and Earth System Sciences* 22, 1–25.

Régnier, J., Bonilla, L., Bard, P., Bertrand, E., Hollender, F., Kawase, H., Sicilia, D., Arduino, P., Amorosi, A., Asimaki, D., Boldini, D., Chen, L., Chiaradonna, A., DeMartin, F., Elgamal, A., Falcone, G., Foerster, E., Foti, S., Garini, E., Gazetas, G., Gélis, C., Ghofrani, A., Giannakou, A., Gingery, J., Glinsky, N., Harmon, J., Hashash, Y., Iai, S., Kramer, S., Kontoe, S., Kristek, J., Lanzo, G., Lernia, A. di, Lopez‐Caballero, F., Marot, M., McAllister, G., Diego Mercerat, E., Moczo, P., Montoya‐Noguera, S., Musgrove, M., Nieto‐Ferro, A., Pagliaroli, A., Passeri, F., Richterova, A., Sajana, S., Santisi d'Avila, M.P., Shi, J., Silvestri, F., Taiebat, M., Tropeano, G., Vandeputte, D., Verrucci, L. (2018). PRENOLIN: International Benchmark on 1D Nonlinear Site‐Response Analysis−Validation Phase Exercise. *Bulletin of the Seismological Society of America* 108, 876‐900.

Rizzitano, S., Cascone, E., Biondi, G. (2014). Coupling of topographic and stratigraphic effects on seismic response of slopes through 2D linear and equivalent linear analyses. *Soil Dynamics and Earthquake Engineering* 67, 66–84.

Schanz, T., Vermeer, P.A., Bonnier, P.G. (1999). The hardening soil model: Formulation and verification. Beyond 2000 in computational geotechnics. *Ten Years of PLAXIS International. Proceedings of the international symposium*, Amsterdam, March 1999. 281–296.

Stucchi, M., Meletti, C., Montaldo, V., Crowley, H., Calvi, G.M., Boschi, E. (2011). Seismic Hazard Assessment (2003–2009) for the Italian Building Code. *Bulletin of the Seismological Society of America* 101, 1885–1911.

Zhu, C., Cotton, F., Kawase, H., Nakano, K. (2022). How well can we predict earthquake site response so far? Machine learning vs physics-based modeling. *Earthquake Spectra*.